Assessment of pulmonary perfusion with breath-hold and free-breathing dynamic contrast-enhanced magnetic resonance imaging: quantification and reproducibility

Michael Ingrisch[1], Daniel Maxien[2], Felix Schwab[1], Maximilian F. Reiser[1,2], Konstantin Nikolaou[2], Olaf Dietrich[1]

[1] Josef Lissner Laboratory for Biomedical Imaging, Institute for Clinical Radiology, Ludwig-Maximilians-University Hospital Munich, Germany

[2] Institute for Clinical Radiology, Ludwig-Maximilians-University Hospital Munich, Germany

ELECTRONIC PREPRINT VERSION:
This is a non-final version of an article published in final form in Investigative Radiology.
Invest Radiol 2014; **49**(6): 382–389 <URL:http://dx.doi.org/10.1097/RLI.0000000000000020>.

Abstract

Objectives: The purpose of this study was to investigate whether quantification of pulmonary perfusion from dynamic contrast-enhanced (DCE) MRI yields more reproducible results with data acquired during free breathing than with data from conventional breath-hold measurements.

Material and Methods: 10 healthy male volunteers underwent two imaging sessions at a clinical 1.5T-MRI system, separated by a week ± one day. Each of these sessions comprised two DCE MRI acquisitions, one performed during breath-hold, and one during free, shallow breathing; both acquisitions were separated by at least 20 minutes. For all DCE MRI measurements, a standard dose of Gadobutrol was used. Breath hold measurements lasted 53 seconds; free-breathing acquisitions were performed in a total acquisition time of 146 seconds.

Lung tissue was segmented automatically to minimize user influence and pulmonary plasma flow (PPF) and volume (PPV) were quantified on a per-pixel basis with a one-compartment model. Free-breathing measurements were analyzed twice, (a) including data from the entire acquisition duration and (b) after truncation to the duration of the breath-hold measurements. For further statistical analysis, median values of the resulting parameter maps were determined. To assess intra-individual reproducibility, intra-class correlation coefficients and coefficients of variation between first and second measurements were calculated for breath-hold, truncated and full free-breathing measurements, respectively. Differences in the coefficients of variation were assessed with a non-parametric two-sided paired Wilcoxon signed-rank test.

Results: All 40 measurements were completed successfully. Maps of PPF and PPV could be calculated from both measurement techniques; PPF and PPV in the breath-hold measurements were significantly lower ($p<0.001$) than in truncated and full free-breathing measurements. Both evaluations of the free-breathing measurements yielded higher intra-class correlation coefficients and lower coefficients of variation between first and second measurements than in the breath-hold measurements.

Conclusions: Besides offering substantially higher patient comfort, free-breathing DCE MRI acquisitions allow for pixel-wise quantification of pulmonary perfusion and hence generation of parameter maps. Moreover, quantitative perfusion estimates derived from free-breathing DCE MRI measurements have better reproducibility than estimates from the conventionally used breath-hold measurements.

Keywords:

DCE MRI, Pulmonary perfusion, Free breathing, Quantification

Corresponding Author:

Michael Ingrisch, PhD
Institute for Clinical Radiology, Ludwig-Maximilians-University Hospital Munich, Marchioninistr. 15, 81377 Munich, GERMANY
Phone: +49 89 7095-4622, Fax +49 89 7095-4627
E-mail: michael.ingrisch@med.lmu.de

Introduction

Pulmonary perfusion can be assessed qualitatively [1-4] and quantitatively [4-12] by dynamic contrast-enhanced magnetic resonance imaging (DCE MRI). In such an experiment, contrast agent (CA) is administered intravenously as a bolus; subsequently, the spatial and temporal distribution of the CA in the tissue is monitored using an appropriate fast imaging sequence. From the measured signal intensities, the time-resolved contrast-agent concentrations in each voxel can be estimated and further analyzed using tracer-kinetic theory [13], with the objective to derive physiological parameters such as pulmonary plasma flow (PPF) or pulmonary plasma volume (PPV).

Measurements of pulmonary perfusion are usually performed during breath hold, in order to avoid or at least to minimize the detrimental effects of breathing-related motion on the quantification. Breath-hold measurements are intrinsically limited to rather short total acquisition times of typically substantially less than one minute and obviously have poor patient compliance – to the extent that patients often are unable to hold their breath long enough to complete the entire measurement. Moreover, it has been shown that pulmonary perfusion depends strongly on the degree of inspiration, with perfusion in inspiration being significantly lower than perfusion in expiration [8]. Since the level of inspiration at which a breath hold is performed is difficult to control [14], this effect contributes to poor intra-individual reproducibility of quantitative estimates of PPF and PPV.

An acquisition during free breathing is desirable to circumvent these limitations. Such an acquisition technique leads to measurements averaged over the entire breathing cycle, as well as to an increased patient compliance. The feasibility of a free-breathing acquisition for the quantification of pulmonary perfusion during free shallow breathing has recently been demonstrated [15].

Performing the pulmonary perfusion measurement during free breathing inevitably leads to artifacts in perfusion parameter maps, particularly in areas close to lung boundaries (such as the diaphragm) with relatively strong breathing-related movement. However, by averaging over the entire breathing cycle, estimates of pulmonary perfusion in less motion-affected areas of the lung might be more stable and hence more reproducible. Therefore, we hypothesize that a DCE MRI measurement of pulmonary perfusion during free, shallow breathing yields more reproducible measures of pulmonary perfusion than a measurement during breath-hold. In this study, we investigate this hypothesis in a volunteer study, in which we compare free-breathing and breath-hold measurements of pulmonary perfusion.

Materials and Methods

Volunteers and study design

The study protocol of the volunteer study had been approved by the institutional ethics committee. Ten healthy, male volunteers without any symptoms or previous medical history of chest disease (median age 30 years, range 25-39 years) underwent two MR imaging sessions, separated by one week ± one day. Informed consent was obtained from all volunteers. Inclusion criteria were male gender, health and non-smoking. In each imaging session, two dynamic contrast-enhanced measurements were performed, one during breath hold (BH) and one during free, shallow breathing (FB). The two acquisitions were separated by 20 minutes to minimize the influence of residual contrast agent from the first measurement. The order of FB and BH measurements was randomized between volunteers, but kept constant between the first and second imaging session in the same volunteer.

DCE MRI measurements

All MR examinations were performed on a 1.5 T whole-body MRI system (Magnetom Aera, Siemens Healthcare, Erlangen, Germany). For signal reception, a 16-channel spine array coil and an 18-channel body matrix coil were used. For the dynamic acquisition, a 3D spoiled-gradient echo sequence (TWIST), accelerated with parallel imaging and view sharing [16, 17], was optimized to acquire a series of coronal volumes (phase-encoding: LR) covering the chest in 1.3 seconds per volume. Detailed sequence parameters are given in Table 1. Almost all acquisition parameters were kept constant for free-breathing and breath-hold acquisitions, the only difference being the number of acquired volumes and hence the total acquisition time: In the breath-hold meas-

urements, 40 volumes were acquired in a total acquisition time of 53 seconds. Not being restricted to one breath hold, free-breathing measurements were carried out over 146 seconds and acquired 110 consecutive volumes, thus enabling evaluations either of the same duration as the breath-hold measurements by truncating the data sets, or of the longer full duration to potentially benefit from the larger amount of available data.

For the breath-hold measurements, volunteers were instructed to hold their breath as long as possible in half expiration and to continue with shallow breathing, if necessary. Shallow breathing throughout the entire acquisition time was required from the volunteers during the free-breathing measurements.

Both for free-breathing and breath-hold measurements, a body-weight adapted dose of 0.1 mmol/kg body weight of contrast agent (gadobutrol, Gadovist, Bayer Healthcare, Berlin, Germany) was injected with a power injector in the antecubital vein with a flow rate of 3 ml/s, followed by a saline flush of 25 ml with the same flow rate. The injection was started simultaneously with the start of the acquisition.

Table 1: Sequence parameters

	Breath hold	Free breathing
TE / TR	0.9 ms / 2.0 ms	
Matrix size	128×128×36	
Spatial resolution	3×3×4 mm³	
Temporal resolution	1.3 s	
Flip angle	15°	
Bandwidth	1115 Hz/px	
TWIST: pA / pB	0.21 / 0.26	
Parallel imaging	GRAPPA, *R*=2, 24 reference lines	
Total acquisition time	53 s	146 s
Acquired volumes	40	110

Post-processing

The measured data was imported into in-house developed software (PMI 0.4, [18]) written in IDL; all post-processing was performed within this software.

Measurement of the arterial input function

The arterial input function was measured in the pulmonary artery. In order to maximize reproducibility and to minimize user influence, user input was reduced to the definition of a region close to the branch of the pulmonary artery. Within this region, the pixel values were averaged for each time point. The arrival time of contrast agent in the pulmonary artery was determined by inspection of the time intensity curve in the arterial region, and the baseline signal S_0 was determined by temporal averaging over all timepoints before the arrival of contrast agent. Contrast agent concentration in this region was then calculated using the absolute signal enhancement $S(t) - S_0$. To derive the concentration in blood plasma, the arterial signal enhancement curve was rescaled with 1/(1-hct), where hct denotes the hematocrit value. Since no individual hematocrit values were available, a fixed value of the hct=0.45 was assumed.

Automatic segmentation

Contrast agent concentrations in each pixel curve were also calculated from the absolute signal enhancement $S(t) - S_0$. The arterial input function was used for automatic segmentation of the lung tissue in the entire dataset (excluding large vessels, image background and other tissue) as described previously [7]. In summary, a map of the cross correlation of each pixel concentration-time course with the AIF was calculated; all pixels with cross correlation values over 0.3 (to exclude non-lung tissue) and below 0.9 (to exclude voxels in pulmonary arteries) were included in a region. Moreover, a map of the area under the curve, normalized to the area under the AIF (nAUC), was calculated, all pixels with nAUC values below 0.05 (to exclude background pixels) and higher than 0.5 (to exclude pixels in blood vessels) were excluded from the final lung tissue region.

Quantification

Pulmonary perfusion was quantified from the breath-hold measurement, from the entire free breathing measurement and, to ensure comparability between breath-hold and free-breathing measurements, from the free-breathing meas-

urement truncated to the first 40 time frames, thus corresponding to the same total acquisition time as used in the breath-hold measurement.

To each signal enhancement curve $S(t)-S_0$ in the previously defined region, a one-compartment model [6, 13, 19] was fitted, yielding maps of PPF and PPV. The median values of these maps were then used as surrogate markers of pulmonary perfusion and used for further statistical analysis.

Statistical analysis

Statistical analysis was performed in R [20]. Differences in PPF and PPV between breath-hold and full free-breathing measurements as well as between breath-hold and truncated free-breathing measurements were assessed with non-parametric, paired two-sided Wilcoxon signed rank tests. Since the truncated and full free-breathing data do not represent statistically independent samples, testing for differences between these data was not performed.

In order to assess the test-retest reproducibility of free-breathing and breath-hold pulmonary perfusion measurements, the two-way agreement intraclass correlation coefficients (ICC) of first and second volunteer measurements were calculated using the R package 'irr' [21]. Additionally, the intra-individual coefficients of variation (CV) between these measurements were calculated. Differences in CV between breath-hold and truncated free-breathing measurements as well as between breath-hold and full free-breathing measurements were assessed with non-parametric, paired two-sided Wilcoxon signed rank tests. Reproducibility was determined as the root mean square average over all coefficients of variation for free-breathing and breath-hold measurements [22]; 95% confidence intervals were calculated with the bootstrap method [23].

Results

All 40 measurements were completed successfully and no adverse events were observed. The baseline time before arrival of contrast agent in the pulmonary artery was in the range of 3 to 9 time frames. Segmentation of pulmonary parenchyma produced regions that contained mainly pulmonary parenchyma in all volunteers. In all regions, the segmentation algorithm reliably excluded large arterial and venous vessels. Regions close to the diaphragm, where most of the breathing-related motion occurred, were excluded as well. Fine-tuning of the thresholds was not required in any of the datasets. Figure 1 demonstrates key steps of the segmentation algorithm in an exemplary slice of a free-breathing dataset. The evaluated volume in the maps obtained from the free-breathing data (mean/sd 2.3l/0.58l), was significantly ($p<0.001$) smaller than the corresponding volume from breath-hold data (mean/sd 3.3l/0.71l).

Fig. 2a displays representative maps of PPF from two volunteers, calculated from the breath-hold, truncated and full free-breathing measurements, respectively. Maps from both measurements demonstrate that the segmentation algorithm selected mainly voxels in lung tissue, with the exception of some single voxels. Fig. 2b shows the corresponding maps of PPV.

Median values of PPV and PPF of all 40 measurements are shown in Table 2 and Fig. 3. No significant differences ($p>0.05$) between first and second measurements were observed for either parameter in breath-hold and free-breathing measurements. Table 3 displays the overall mean values of PPF and PPV, averaged over first and second measurement. PPF and PPV are significantly ($p<0.001$) higher (by 25 to 37%) in truncated and full free-breathing measurements than in the breath-hold measurements, while the relative difference between truncated and full free-breathing measurements, on the other hand, is only 5.4% for PPF and 4.0% for PPV.

Intra-class correlations of PPV between baseline and follow-up measurements were significant ($p<0.01$) both for breath-hold, truncated and full free-breathing measurements; PPF ICC was only significant ($p<0.005$) for the free-breathing measurements and non-significant ($p>0.05$) for the breath-hold measurement. ICC values, together with the corresponding p-values are displayed in Table 4. Intra-class correlation was higher for free-breathing than for breath-hold, and higher for PPV than for PPF.

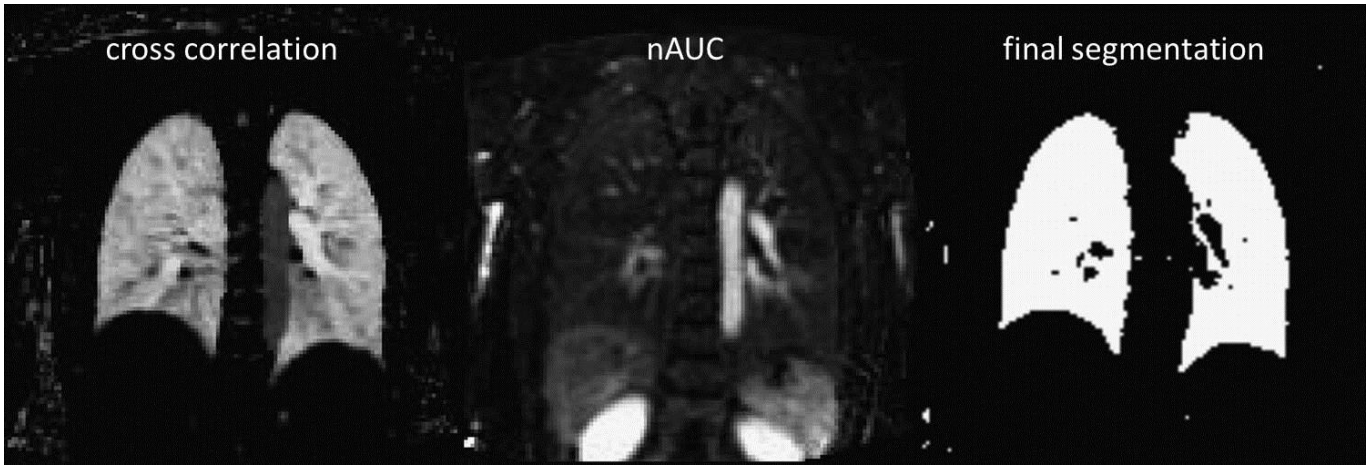

Figure 1: Segmentation. Key steps of the segmentation algorithm: The left image displays the cross correlation of each voxel with the arterial input function, measured in the pulmonary artery. Lung arteries and lung parenchyma have the best cross correlation, whereas the cross correlation with all other tissues and vessels is much smaller. The center image shows the corresponding map of the normalized area under the curve; the right image is the final segmentation, resulting from thresholding of the two parameter maps.

Table 2: Quantitative values. Values of quantitative perfusion parameters in all measurements. Pulmonary plasma flow (PPF) is given in ml/100ml/min, pulmonary plasma volume (PPV) in ml/100ml.

		Breath hold		Truncated free breathing		Free breathing	
Parameter	volunteer	first measurement	second measurement	first measurement	second measurement	first measurement	second measurement
PPF	1	208.3	186.3	281	237	267.3	227.5
	2	172.9	114.7	325	297	311.6	275.3
	3	166.6	202.4	140	180	136.4	174.1
	4	301.4	218.7	331	283	317.3	267.6
	5	116.1	125.4	159	166	144.6	158.9
	6	122.3	94.3	132	137	124.1	131.4
	7	112.3	201.1	329	282	188.9	267.1
	8	453.9	227.1	518	329	491.6	301.2
	9	190.8	122.3	169	145	164.8	140.2
	10	216.9	89.6	275	293	259.5	279.2
	Mean	**206.2**	**158.2**	**266**	**235**	**240.6**	**222.3**
	SD	**94.1**	**48.7**	**109**	**65**	**103.2**	**58.6**
PPV	1	12.4	10.0	14.0	12.6	15.3	14.8
	2	7.9	7.9	13.8	15.0	14.6	17.9
	3	9.6	8.3	10.4	10.1	10.7	10.4
	4	16.3	16.4	17.1	14.1	18.5	14.8
	5	7.8	10.5	8.3	11.0	8.8	11.6
	6	7.5	6.0	8.4	8.2	7.7	7.9
	7	7.5	9.4	10.8	10.7	10.9	10.3
	8	12.0	9.6	17.4	14.7	17.2	15.2
	9	11.1	7.6	9.0	8.0	8.5	8.1
	10	10.0	6.6	14.7	13.3	15.0	13.9
	Mean	**10.2**	**9.2**	**12.4**	**11.8**	**12.7**	**12.5**
	SD	**2.6**	**2.6**	**3.1**	**2.3**	**3.5**	**3.0**

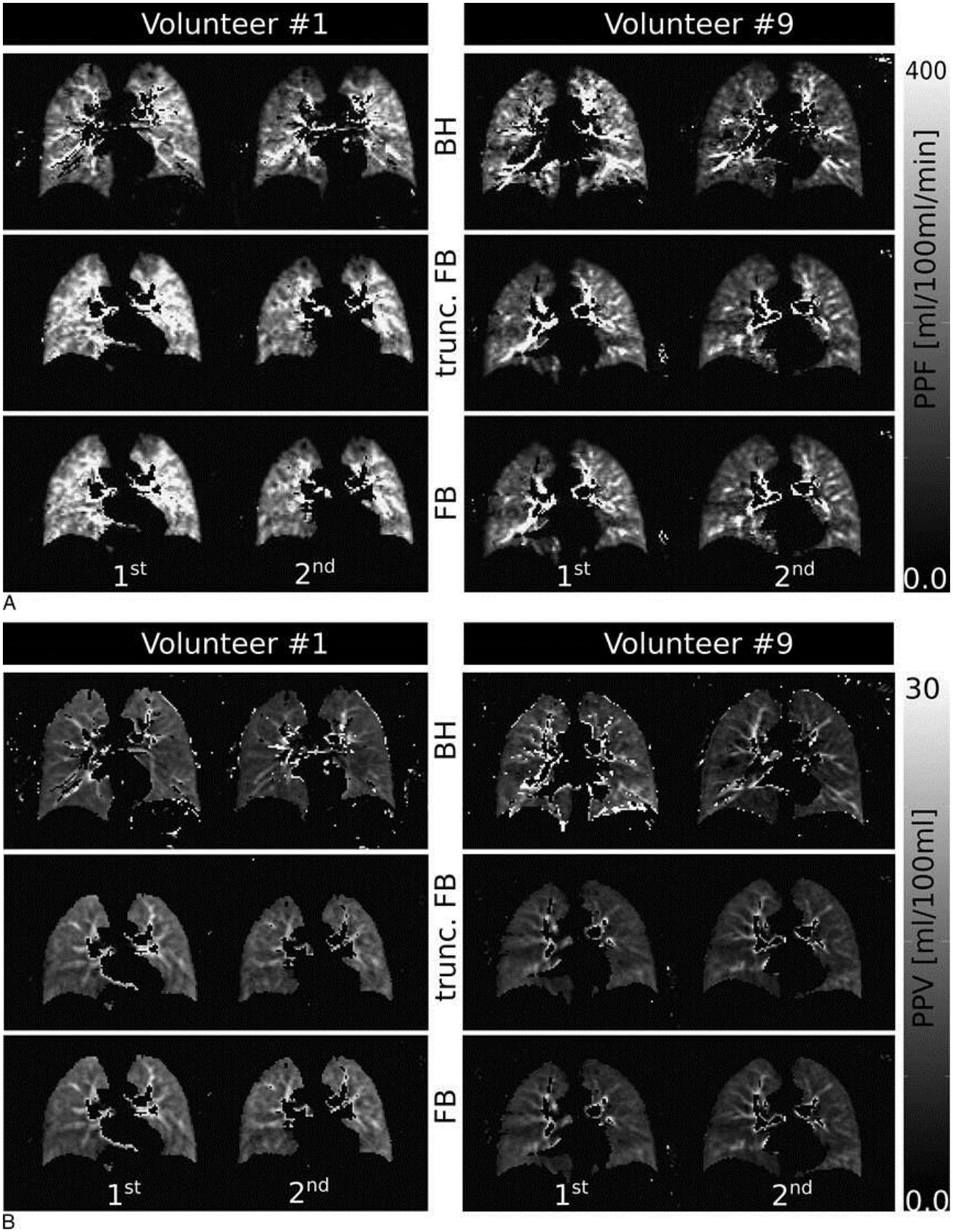

Figure 2: Parameter maps. A) PPF maps of a representative slice (#20) from two volunteers (#1 and #9), comparing first and second measurements of breath hold, truncated and full free-breathing. All maps display the PPF range from 0 to 400 ml/100ml/min, as indicated by the color bar. B) Corresponding PPV map of the same slice in the same volunteers. All maps display the PPV range from 0 to 30 ml/100ml.

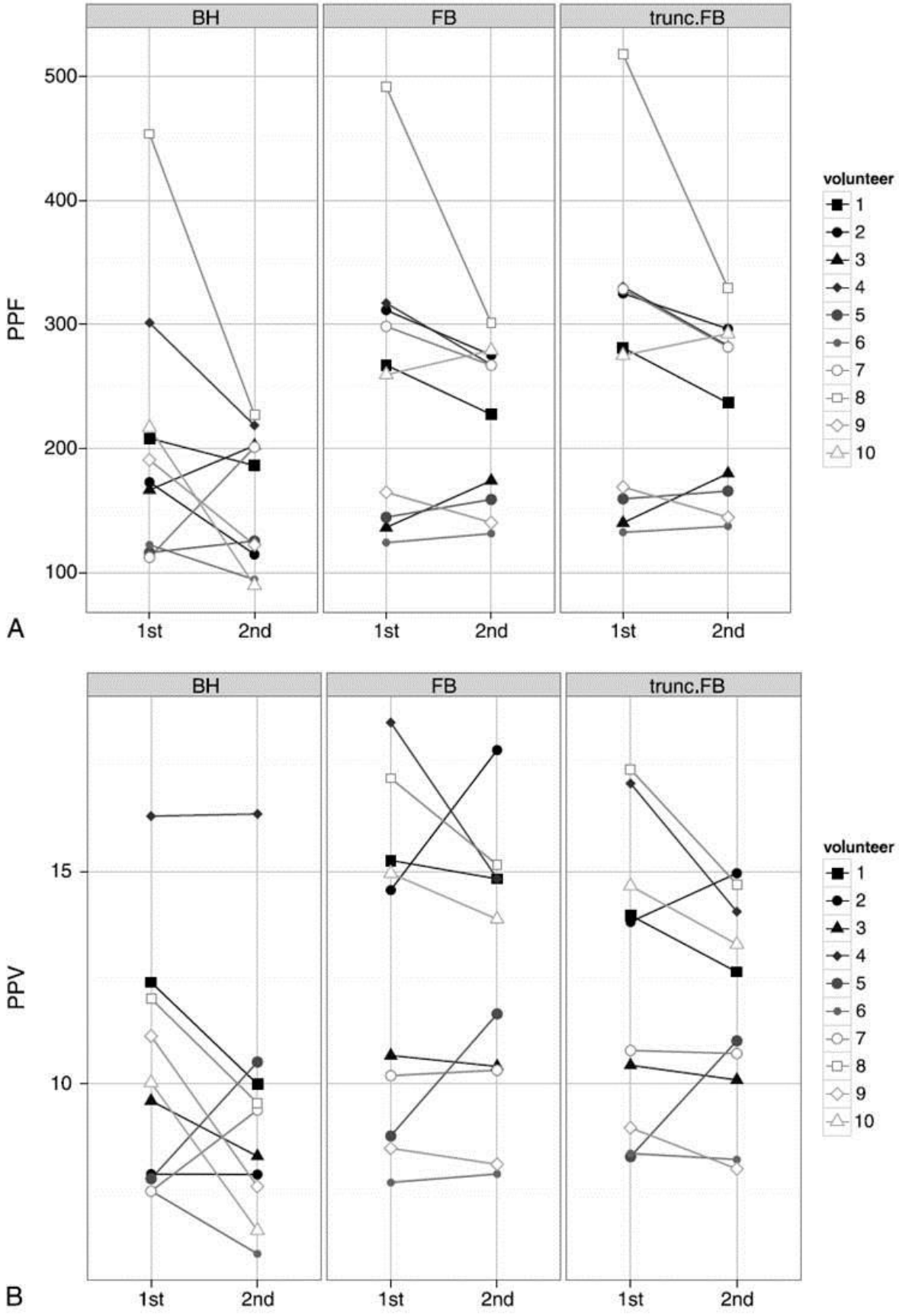

Figure 3: Overview over quantitative results. A) Top row: Quantitative estimates of PPF for breath-hold, full and truncated free-breathing measurements; first and second measurements in each volunteer are connected. B) Bottom row: Corresponding results for PPV estimates

Table 3: Overall mean values of PPF and PPV

	BH	Truncated FB	FB
PPF [ml/100ml/min]	182.2	250.3	236.9
PPV [ml/100ml]	9.7	12.6	12.1

Table 4: ICC and reproducibility

Parameter	Mode	ICC	p	CV (RMS)	Confidence interval	
PPF	Breath hold	0.39	0.085	0.32	0.22	0.43
	Trunc. free breathing	0.77	0.002	0.14	0.08	0.20
	Free breathing	0.74	0.003	0.14	0.08	0.21
PPV	Breath hold	0.70	0.005	0.18	0.13	0.23
	Trunc. free breathing	0.84	0.006	0.10	0.06	0.14
	Free breathing	0.85	0.003	0.10	0.06	0.15

Intra-class correlation coefficients with the corresponding p-values, test-retest reproducibility (RMS, root mean square average of CV values; a lower value indicates better reproducibility) and 95% confidence intervals of RMS of PPF and PPV both for breath-hold, truncated free breathing and free-breathing measurements.

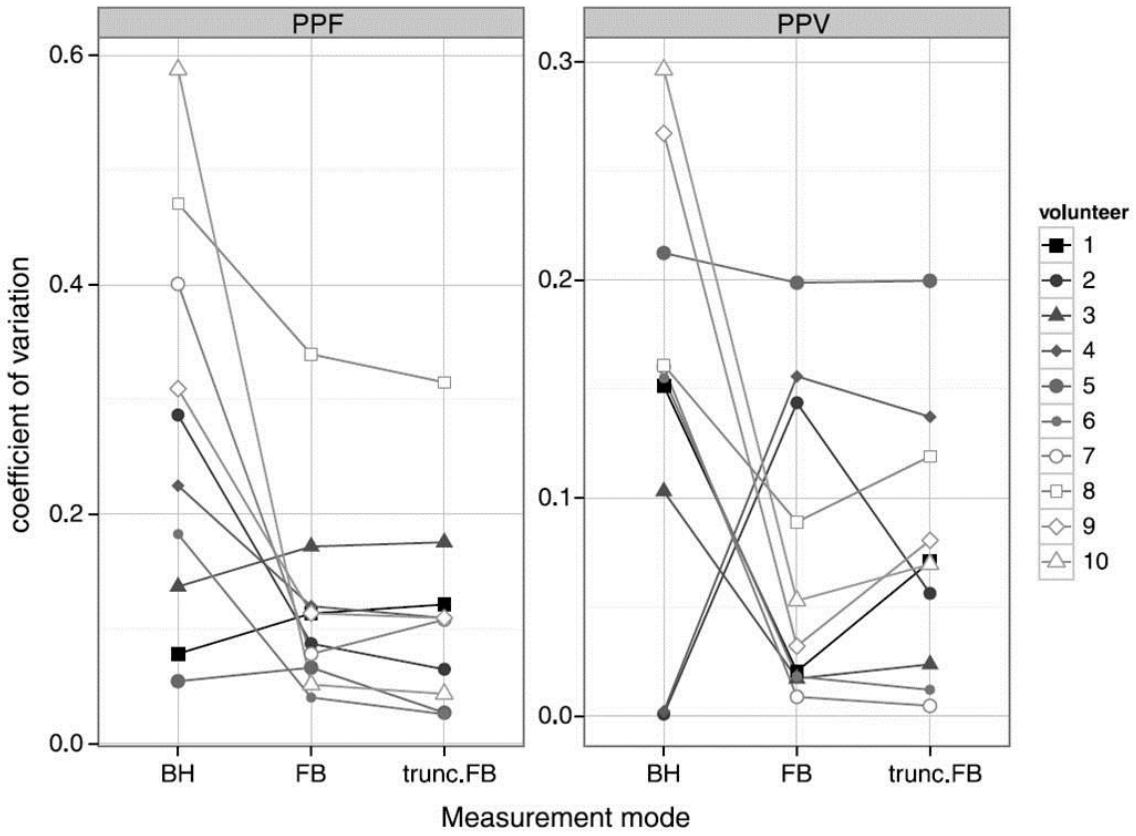

Figure 4: Coefficients of variation. Coefficients of variation for the breath-hold, truncated and full free-breathing measurements: free-breathing measurements yield lower coefficients of variation for PPF and PPV, indicating better reproducibility than the conventional breath-hold acquisitions.

The coefficients of variation are shown in Fig. 4 for PPF (left) and PPV (right). Coefficients of variation of truncated and full free-breathing measurements were significantly lower ($p<0.05$) than those of the breath-hold measurements for PPF and lower, although not significantly ($p>0.05$), for PPV. Reproducibility, assessed as the root-mean-square average of the coefficients of variation, is also given in Table 4, along with bootstrapped 95% confidence intervals; reproducibility is much better for truncated and full free-breathing measurements than for breath-hold measurements.

Discussion and conclusion

The feasibility of pulmonary perfusion quantification from free-breathing acquisitions has recently been demonstrated [15]. DCE acquisitions during free breathing are particularly attractive for clinical applications, since they offer substantially increased patient comfort and compliance. Moreover, since the total acquisition time is not limited to a single breath hold, it becomes possible to measure not only vascular parameters like pulmonary plasma flow and volume, but also additional parameters that characterize potential contrast agent extravasation in focal pathologies [13, 24] . A very promising aspect of free breathing pulmonary DCE measurements is that they might allow for a more reproducible assessment of pulmonary hemodynamics due to the intrinsic averaging over the breathing cycle.

Quantification of pulmonary perfusion with standard breath-hold acquisitions has a relatively poor reproducibility due to a combination of several facts: Physiologically, pulmonary perfusion varies strongly throughout the breathing cycle [8], and achieving consistent breath hold in the same phase of the breathing cycle is challenging. Also, quantitative estimates depend critically on the region in which they are evaluated. The often-used region-based approach, in which the concentration time courses of all pixels in a user-defined region are averaged to increase signal-to-noise ratio, is valid only when the region is carefully defined in tissue with homogeneous blood flow and volume. Averaging over an inhomogeneous region such as the lung yields distorted estimates that are strongly influenced by the pixels that contain large vessels. Consequently, the definition of the region in which perfusion is to be assessed is a highly relevant factor for the outcome of such an analysis; if this region is defined manually, this step of region definition introduces strong user dependence.

We aimed to minimize user influence and potential user bias by using an automatic segmentation approach for the definition of regions in lung tissue. Effectively, user input was reduced to the definition of a small region in a well-defined location in the pulmonary artery and the counting of time frames until contrast agent arrived in this region. With this, the post-processing proceeded automatically, so that we assume that user influence plays a small, if not even negligible, role in our quantification of pulmonary perfusion – both for breath-hold and free-breathing data. Our segmentation algorithm was designed to select the entire lung with its rather heterogeneous distribution of perfusion (see Figs. 1 and 2). It is worth mentioning that the algorithm performs even better with longer acquisition times. This can be appreciated in Fig. 2: in the breath-hold datasets, much more background pixels are selected erroneously than in the free-breathing datasets, which were both segmented using the full non-truncated free-breathing data sets. The reason for this behavior is most likely that the free-breathing data is measured over a longer total acquisition time and hence contains more information. Due to this increased informational content, background pixels have poorer cross correlation with the arterial curve and lower values of nAUC, so that a misclassification is less likely than with the shorter breath-hold measurement.

Since averaging over all pixel curves in this region in order to increase the SNR is not a valid option for further quantification, we quantified pulmonary perfusion on the pixel level with a one-compartment model. A model-based approach is favorable in situations with low SNR, since it reduces the number of free parameters to the absolute minimum; whereas the often used deconvolution approaches are known to perform poorly in settings with low SNR [7, 25]. A pixel-based approach has the additional benefit of producing parameter maps instead of mere numbers, so that potential focal perfusion defects can be detected easily.

Quantification and reproducibility

In concordance with a previous study [15] we observed higher values of PPF and PPV in the free-breathing measurement. The reason for this apparently increased perfusion is probably that both PPF and PPV are parameters normalized to volume. Since the average lung volume is smaller in a free-breathing measurement, higher values of the perfusion parameters ensue.

Breathing-induced motion influences the signal intensity in two ways: First, breathing results in fluctuations of lung density and therefore of MR signal. In expiration, the lung volume is smaller and the tissue density and hence the MR signal is higher, whereas in inspiration, tissue density and MR signal are lower. Second, and possibly more important, breathing-induced motion leads to variations in signal intensity, since e.g. small vessels move in and out of each voxel. Since the AIF is not affected by either of these effects, the model fitting process intrinsically averages over the breathing-induced signal fluctuations. After model fitting, these signal fluctuations should result mainly in an increase of the residual sum of squares (χ^2) and only to a lesser extent, if at all, in a change of parameter estimates.

With the influence of the user on the quantification minimized, we were able to demonstrate that free-breathing measurements yield better intra-individual reproducibility of the global values of PPF and PPV than the conventionally used breath-hold measurements – even when evaluated over the same short acquisition time. The reason for this better reproducibility may be found in the fact that a measurement during free breathing inherently averages over the entire breathing cycle, instead of representing one phase only, such as in- or expiration. However, applied to patients with focal perfusion defects, this smoothing effect might obscure the detectability of very small lesions on parameter maps. It is worth mentioning that a free-breathing measurement allows for longer total acquisition times than a breath-hold measurement. Although not required for the quantification of PPF and PPV, this opens up the possibility to assess and characterize slower processes such as the extravasation of contrast agent, e. g., in tumors.

Interestingly, we observed that pulmonary perfusion in the second breath-hold measurement was lower, although not significantly, than in the first breath-hold measurement. The reason for this effect may be that we demanded a rather long breath hold of 53 seconds. We speculate that, in the second measurement, the volunteers involuntarily hold their breath in deeper inspiration in order to better accomplish this long breath-hold period; the deeper inspiration may be the cause for the lower values of PPF and PPV. Although this trend of lower pulmonary perfusion in the second measurement was non-significant, this systematic effect obviously impedes the reproducibility of the breath-hold measurements. Better training of the breath hold prior to the MR examination might therefore improve the reproducibility of breath-hold measurement. Nevertheless, in a clinical setting, a free-breathing measurement without the need for additional training might be preferable.

Further observations and potential improvements: dealing with motion

It is worth mentioning that the reproducibility of free breathing pulmonary perfusion MRI might be increased even further by more elaborate means of dealing with diaphragm motion. A possible strategy for this purpose is retrospective triggering, e.g. on the diaphragm position [26], and discarding, e. g., all volumes acquired during ex- or inspiration. However, this strategy significantly reduces the effective temporal resolution. This entails that rapid signal changes, which occur e.g. during the first passage of the contrast agent, are missed, which is detrimental for the quantification of PPF.

A more refined, but also more challenging method would be to use an elastic registration of consecutive time frames to a reference image [27] . This strategy requires additional and complex post-processing; a particular challenge is the differentiation of rapid signal changes that are due to passage of contrast agent from signal changes that are due to motion. Nevertheless, this approach might be beneficial for datasets with more breathing-related motion than in our study, e.g. in patient measurements.

Limitations of this study

Our study is not without limitations. First of all, only a small number of healthy volunteers were

included in the study. Results in patients, potentially with lung diseases, may differ from the results found in this study, in particular, if the patients are unable to breathe as shallowly as the volunteers in this study. It remains to be investigated in further studies with different patient cohorts, whether the promising results of this study can be translated into clinical practice. However, we expect no fundamental problems of the free-breathing protocol, especially in the light of the much better patient compliance of a free-breathing acquisition.

For each contrast-enhanced measurement, a standard dose of contrast agent was injected with a flow of 3 ml/s. This causes a high concentration of contrast agent, in particular during the first pass of contrast agent through the pulmonary artery. It may well be that the linearity regime of the acquisition is exceeded here, leading to an underestimation of the arterial concentration. This would cause an overestimation of PPF and PPV. However, we did not observe signal saturation or flattening of the arterial peak during the first pass, and the observed perfusion parameters are well within the range known from literature. A pre-bolus measurement [28, 29] would be very helpful in removing the effects of potential nonlinearities, but was not performed in this study. Nevertheless, the objective of this study was the assessment of reproducibility of quantitative pulmonary perfusion by comparison of two measurements separated by one week. Since the protocol was unchanged, potential nonlinearities would have affected both measurements in the same manner, so that we assume that they do not play a significant role for the assessment of reproducibility.

In our study, two doses of contrast agent were applied in each imaging session; the time interval between the two injections was 20 minutes or longer. Although we cannot entirely exclude the possibility that residual contrast agent from the first injection might influence the second measurement, this should not affect the assessment of reproducibility, since the order of FB and BH acquisitions within each volunteer was the same in each imaging session and randomized only inter-individually.

In conclusion, we were able to demonstrate that pulmonary perfusion in healthy volunteers can be quantified more reproducible from measurements obtained during free breathing than from measurements during breath hold. This is a very encouraging result, since free-breathing measurements are easier to implement in clinical routine than the conventionally used breath-hold measurements, which pose higher demands both on technician and on the patient.

References

1. Dehnert C, Risse F, Ley S, et al. Magnetic resonance imaging of uneven pulmonary perfusion in hypoxia in humans. American journal of respiratory and critical care medicine. 2006;174:1132-8. doi:10.1164/rccm.200606-780OC.

2. Fink C, Puderbach M, Bock M, et al. Regional lung perfusion: assessment with partially parallel three-dimensional MR imaging. Radiology. 2004;231:175-84. doi:10.1148/radiol.2311030193.

3. Fink C, Bock M, Puderbach M, et al. Partially parallel three-dimensional magnetic resonance imaging for the assessment of lung perfusion--initial results. Invest Radiol. 2003;38:482-8. doi:10.1097/01.rli.0000067490.97837.82.

4. Hueper K, Parikh MA, Prince MR, et al. Quantitative and semiquantitative measures of regional pulmonary microvascular perfusion by magnetic resonance imaging and their relationships to global lung perfusion and lung diffusing capacity: the multiethnic study of atherosclerosis chronic obstructive pulmonary disease study. Invest Radiol. 2013;48:223-30. doi:10.1097/RLI.0b013e318281057d.

5. Tomasian A, Krishnam MS, Lohan DG, et al. Adult Tetralogy of Fallot: quantitative assessment of pulmonary perfusion with time-resolved three dimensional magnetic resonance angiography. Invest Radiol. 2009;44:31-7. doi:10.1097/RLI.0b013e31818d385b.

6. Nikolaou K, Schoenberg SO, Brix G, et al. Quantification of Pulmonary Blood Flow and Volume in Healthy Volunteers by Dynamic Contrast-Enhanced Magnetic Resonance Imaging Using a Parallel Imaging Technique. Investigative Radiology. 2004;39:537-45. doi:10.1097/01.rli.0000133813.22873.47.

7. Ingrisch M, Dietrich O, Attenberger UI, et al. Quantitative pulmonary perfusion magnetic resonance imaging: influence of temporal resolution and signal-to-noise ratio. Invest Radiol. 2010;45:7-14. doi:10.1097/RLI.0b013e3181bc2d0c.

8. Fink C, Ley S, Risse F, et al. Effect of inspiratory and expiratory breathhold on pulmonary perfusion: assessment by pulmonary perfusion magnetic resonance imaging. Invest Radiol. 2005;40:72-9.

9. Ley S, Mereles D, Risse F, et al. Quantitative 3D pulmonary MR-perfusion in patients with pulmonary arterial hypertension: correlation with invasive pressure measurements. European journal of radiology. 2007;61:251-5. doi:10.1016/j.ejrad.2006.08.028.

10. Ley S, Fink C, Risse F, et al. Magnetic resonance imaging to assess the effect of exercise training on pulmonary perfusion and blood flow in patients with pulmonary hypertension. European radiology. 2013;23:324-31. doi:10.1007/s00330-012-2606-z.

11. Ohno Y, Koyama H, Yoshikawa T, et al. Contrast-enhanced multidetector-row computed tomography vs. Time-resolved magnetic resonance angiography vs. contrast-enhanced perfusion MRI: assessment of treatment response by patients with inoperable chronic

thromboembolic pulmonary hypertension. Journal of magnetic resonance imaging : JMRI. 2012;36:612-23. doi:10.1002/jmri.23680.

12. Ohno Y, Hatabu H, Murase K, et al. Primary pulmonary hypertension: 3D dynamic perfusion MRI for quantitative analysis of regional pulmonary perfusion. AJR American journal of roentgenology. 2007;188:48-56. doi:10.2214/AJR.05.0135.

13. Ingrisch M, Sourbron S. Tracer-kinetic modeling of dynamic contrast-enhanced MRI and CT: a primer. Journal of pharmacokinetics and pharmacodynamics. 2013;40:281-300. doi:10.1007/s10928-013-9315-3.

14. Plathow C, Ley S, Zaporozhan J, et al. Assessment of reproducibility and stability of different breath-hold maneuvres by dynamic MRI: comparison between healthy adults and patients with pulmonary hypertension. European radiology. 2006;16:173-9. doi:10.1007/s00330-005-2795-9.

15. Maxien D, Ingrisch M, Meinel F, et al. Quantification of Pulmonary Perfusion with Free-Breathing Dynamic Contrast-Enhanced MRI - A Pilot Study in Healthy Volunteers. RoFo : Fortschritte auf dem Gebiete der Rontgenstrahlen und der Nuklearmedizin. 2013. doi:10.1055/s-0033-1350128.

16. Song T, Laine AF, Chen Q, et al. Optimal k-space sampling for dynamic contrast-enhanced MRI with an application to MR renography. Magnetic resonance in medicine : official journal of the Society of Magnetic Resonance in Medicine / Society of Magnetic Resonance in Medicine. 2009;61:1242-8. doi:10.1002/mrm.21901.

17. Attenberger UI, Ingrisch M, Dietrich O, et al. Time-resolved 3D pulmonary perfusion MRI: comparison of different k-space acquisition strategies at 1.5 and 3 T. Invest Radiol. 2009;44:525-31. doi:10.1097/RLI.0b013e3181b4c252.

18. Sourbron S, Biffar A., Ingrisch M., et al. PMI: platform for research in medical imaging. Magn Reson Mater Phy 2009;22:539.

19. Sourbron SP, Buckley DL. Tracer kinetic modelling in MRI: estimating perfusion and capillary permeability. Physics in medicine and biology. 2012;57:R1-33. doi:10.1088/0031-9155/57/2/R1.

20. R: A language and environment for statistical computing. R Foundation for Statistical Computing; 2011.

21. irr: Various Coefficients of Interrater Reliability and Agreement. 2012.

22. Raya JG, Horng A, Dietrich O, et al. Articular cartilage: in vivo diffusion-tensor imaging. Radiology. 2012;262:550-9. doi:10.1148/radiol.11110821.

23. Efron B. Better Bootstrap Confidence-Intervals. J Am Stat Assoc. 1987;82:171-85. doi:Doi 10.2307/2289144.

24. Naish JH, Kershaw LE, Buckley DL, et al. Modeling of contrast agent kinetics in the lung using T1-weighted dynamic contrast-enhanced MRI. Magnetic resonance in medicine : official journal of the Society of Magnetic Resonance in Medicine / Society of Magnetic Resonance in Medicine. 2009;61:1507-14. doi:10.1002/mrm.21814.

25. Murase K, Yamazaki Y, Miyazaki S. Deconvolution analysis of dynamic contrast-enhanced data based on singular value decomposition optimized by generalized cross validation. Magnetic resonance in medical sciences : MRMS : an official journal of Japan Society of Magnetic Resonance in Medicine. 2004;3:165-75.

26. Attenberger UI, Sourbron SP, Michaely HJ, et al. Retrospective respiratory triggering renal perfusion MRI. Acta radiologica. 2010;51:1163-71. doi:10.3109/02841851.2010.519717.

27. Merrem AD, Zollner FG, Reich M, et al. A variational approach to image registration in dynamic contrast-enhanced MRI of the human kidney. Magnetic resonance imaging. 2013;31:771-7. doi:10.1016/j.mri.2012.10.011.

28. Risse F, Semmler W, Kauczor HU, et al. Dual-bolus approach to quantitative measurement of pulmonary perfusion by contrast-enhanced MRI. Journal of magnetic resonance imaging : JMRI. 2006;24:1284-90. doi:10.1002/jmri.20747.

29. Kostler H, Ritter C, Lipp M, et al. Prebolus quantitative MR heart perfusion imaging. Magnetic resonance in medicine : official journal of the Society of Magnetic Resonance in Medicine / Society of Magnetic Resonance in Medicine. 2004;52:296-9. doi:10.1002/mrm.20160.